Spectrogoniometric Measurements And Modeling Of Apollo 11 Soil 10084. J.R. Johnson[1], M.K. Shepard[2], D.A. Paige[3], E.J. Foote[3], and W. Grundy[4], [1]U.S. Geological Survey, 2255 N. Gemini Dr., Flagstaff, AZ 86001, jrjohnson@usgs.gov, [2]Bloomsburg University, Bloomsburg, PA, [3]UCLA, Los Angeles, CA, [4]Lowell Observatory, Flagstaff, AZ

***Introduction*:** Laboratory visible/near-infrared multispectral goniometer observations of Apollo 11 mature mare soil 10084 (splits 161, 2010, 2011) were acquired using the Bloomsburg University Goniometer (BUG) [1-4], with an emphasis on high phase angle observations. These data provided constraints on Hapke radiative transfer models for comparison to similar BUG data acquired of lunar analog soils [5]. Lunar soil 10084 provides "ground truth" for interpretation of lunar surface observations acquired by orbital cameras and spectrometers on past and upcoming lunar missions [6-11].

Observations. Standard BUG measurements are typically acquired at incidence angles of 0-60°, emission angles of 0-80°, and phase angles of 3-140°, comprising 680 measurements per wavelength [1,5]. We acquired multispectral measurements of the 10084 sample at 450, 550 ,700, 750, 850, and 950 nm at these geometries. We also supplemented this geometric coverage by constructing an elongated sample holder for measurements in and perpendicular to the principal plane [11]. These measurements were acquired at 450, 550, 750, and 950 nm, and allowed expanded geometric coverage to incidence angles of 0-75° and phase angles of 3-155°, comprising 769 measurements per wavelength.

Analyses. Hapke models were run using Henyey-Greenstein (HG) phase functions to determine the asymmetry parameter (ξ) for a 1-term HG, and the *b* (asymmetry parameter; narrow scattering lobes=large values) and *c* (backscattering materials=large values) parameters for a 2-term HG [12]. All models included the single scattering albedo (*w*) and macroscopic roughness parameter ($\bar{\theta}$), as well as the opposition effect magnitude (*B0*) and width (*h*). A reduced chi-square (χ_v^2) estimate of goodness of fit was also derived. The error on each fitted parameter was estimated by testing how χ_v^2 changed when a particular parameter was purposely varied from its original best-fit value [5,12,14].

Results. Table 1 lists the 1-term and 2-term HG results for the expanded and standard geometry data sets acquired for sample 10084. Two-term HG models gave the best model fits (as determined by the χ_v^2 value). Figure 1 shows the bidirectional reflectance distribution function (BRDF) phase curves at 450 nm and 750 nm compared to the results of [5] (acquired at 410, 750 nm). Results from both standard and expanded BUG geometries are quite similar. Values of *w* from the 2-term HG models are shown as a function of wavelength in Figure 2. The 10084 sample exhibits the lowest *w* values compared to the analog samples [5], similar to values modeled for the lunar maria from Clementine images by [15]. The 1-term HG asymmetry parameters were negative (back-scattering) for 10084, similar to the analog bulk JSC-1 sample [5]. Likewise, the 2-term HG modeled *b* and *c* values shown in Figure 3 are more backscattering than any of the lunar analog soils, (although close to the results for bulk JSC-1 and FJS-1), and the results from [15]. These values are similar to the experimental results from [13] for agglutinates and clear, rough spheres. Although *B0* values were not well constrained in the models, the *h* values from 1-term HG models were 0.065 ± 0.010, consistent with Clementine model results [15]. This is lower than any of the lunar analog soils [5], suggesting a more porous nature and/or less uniform grain size. $\bar{\theta}$ values were 14° for sample 10084, lower than all lunar analogs except FJS-1 and JSC-1AF [5]. Notably, the addition of the high emission and incidence angle data does not result in appreciable differences in any of the modeled Hapke parameters. Future work may include immature Apollo soil samples and/or those from the highlands.

References: [1] Shepard, M.K., in *Solar System Remote Sensing Symposium*, #4004, LPI, 2002; [2] Johnson, J.R., et al., *JGR*, 111, E12S07, doi:10.1029/2005JE002658, 2006; [3] Johnson, J.R., W.M. Grundy, and M.K. Shepard, *Icarus*, 171, 546-556, 2004; [4] Shepard, M.K., and P. Helfenstein, *JGR*, 112, E03001, 2007; [5] Johnson, J.R. et al., *LPSC XXXIX*, #1331, 2008; [6] Pieters, C. et al., *LPSC XXXVIII*, #1295, 2007; [7] Kieffer, H.. and Stone, T., Astron. J. 129, 2887-2901, 2005; [8] Hillier, J.K., et al., Icarus, 141, 205-225, 1999; [9] Domingue, D., and F. Vilas, LPSC XXXVI, #1978, 2005; [10] Gunderson, K., et al., Plan. Space Sci., 54, 1046-1056, 2006; [11] Foote, E., et al, this volume [12] Johnson, J.R., et al., *JGR*, 111, E02S14, 2005JE002494, 2006; [13] McGuire, A.F., and B.W. Hapke, *Icarus*, 113, 134-155, 1995; [14] Johnson, J.R., et al., LPSC XXXVIII, # 1288, 2007; [15] Hillier, J. et al., Icarus, 205, 1999.

Acknowledgments: We thank the Planetary Geology and Geophysics program, and the Lunar Reconnaissance Orbiter mission for funding, and CAPTEM for access to lunar sample 10084.

Table 1. Hapke scattering parameters for Apollo sample 10084 (expanded geometry set; *standard geometry set in italics*).

Parameter	450 nm	550 nm	750 nm	950 nm
w (HG1)	0.21 (+0.01,-0.01) *0.21 (+0.00,-0.00)*	0.25 (+0.00,-0.00) *0.25 (+0.00,-0.00)*	0.30 (+0.00,-0.00) *0.31 (+0.00,-0.00)*	0.31 (+0.01,-0.00) *0.32 (+0.00,-0.00)*
w (HG2)	0.27 (+0.00,-0.00) *0.26 (+0.03,-0.00)*	0.31 (+0.00,-0.00) *0.31 (+0.01,-0.00)*	0.38 (+0.00,-0.00) *0.38 (+0.00,-0.00)*	0.39 (+0.01,-0.00) *0.40 (+0.00,-0.00)*
$\bar{\theta}$ *(HG1)*	0 (+--,---); *9 (+1,-1)*	7 (+1,-1); *9 (+1,-1)*	7 (+1,-1); *9 (+1,-1)*	2 (+--,---); *9 (+1,-1)*
$\bar{\theta}$ *((HG2)*	14 (+0,-0); *14 (+3,-0)*	14 (+0,-0); *15 (+1,-0)*	14 (+0,-0); *16 (+0,-0)*	14 (+1,-0); *16 (+0,-0)*
h (HG1)	0.050 (+0.056,-0.007) *0.072 (+0.003,-0.005)*	0.070 (+0.004,-0.003) *0.070 (+0.004,-0.003)*	0.071 (+0.003,-0.003) *0.070 (+0.004,-0.003)*	0.070 (+0.022,-0.017) *0.071 (+0. 002,-0.003*
h (HG2)	0.035 (+0.003,-0.001) *0.050 (+0.038,-0.024)*	0.034 (+0.003,-0.001) *0.037 (+0.016,-0.004)*	0.032 (+0.002,-0.001) *0.037 (+0.016,-0.004)*	0.035 (+0.003,-0.004) *0.036 (+0. 002,-0.001)*
B_0 *(HG1)*	1.0 (+--,---); *1.0 (+--,---)*	1.0 (+--,---); *1.0 (+--,---)*	1.0 (+--,---); *1.0 (+--,---)*	1.0 (+--,---); *1.0 (+--,---)*
B_0 *(HG2)*	1.0 (+--,---); *1.0 (+--,---)*	1.0 (+--,---); *1.0 (+--,---)*	1.0 (+--,---); *1.0 (+--,---)*	1.0 (+--,---); *1.0 (+--,---)*
ξ *(HG1)*	-0.109 (+0.040,-0.014) *-0.095 (+0.005,-0.006)*	-0.086 (+0.005,-0.005) *-0.085 (+0.003,-0.005)*	-0.075 (+0.005,-0.004) *-0.075 (+0.005,-0.003)*	-0.071 (+0.022,-0.012) *-0.067 (+0.005,-0.004)*
b (HG2)	0.343 (+0.005,-0.004) *0.323 (+0.023,-0.003)*	0.343 (+0.004,-0.005) *0.337 (+0.003,-0.004)*	0.343 (+0.005,-0.004); *0.341 (+0.004,-0.003)*	0.338 (+0.009,-0.002) *0.349 (+0. 004,-0.004)*
c (HG2)	0.309 (+0.007,-0.007) *0.324 (+0.007,-0.034)*	0.299 (+0.007,-0.005) *0.302 (+0.002,-0.028)*	0.293 (+0.007,-0.005) *0.281 (+0.005,-0.005)*	0.290 (+0.006,-0.010) *0.260 (+0. 005,-0.005)*
χ_v^2 *(HG1)*	0.02; *0.02*	0.03; *0.03*	0.04; *0.04*	0.04; *0.04*
χ_v^2 *(HG2)*	0.00; *0.00*	0.00; *0.00*	0.01; *0.01*	0.01; *0.01*

HG1, HG2 = 1-term or 2-term Henyey-Greenstein phase functions used; "(+ --,---)" parameter is under-constrained by data

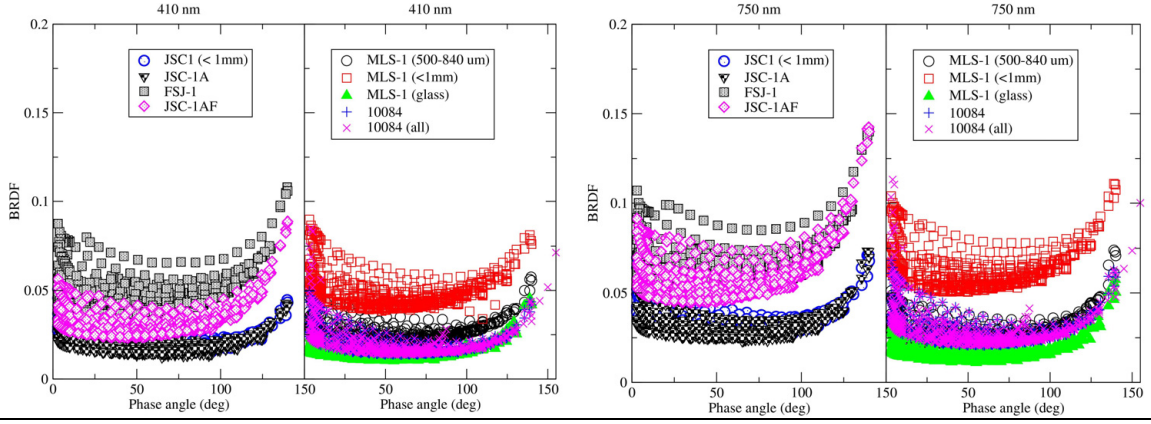

Fig. 1. Bidirectional reflectance distribution function (BRDF) phase curves for analog soils [5] and sample 10084 soils modeled from standard BUG geometries (blue crosses) and from expanded geometries (magenta Xs). Analogs acquired at 410,750 nm; 10084 acquired at 410,750 nm.

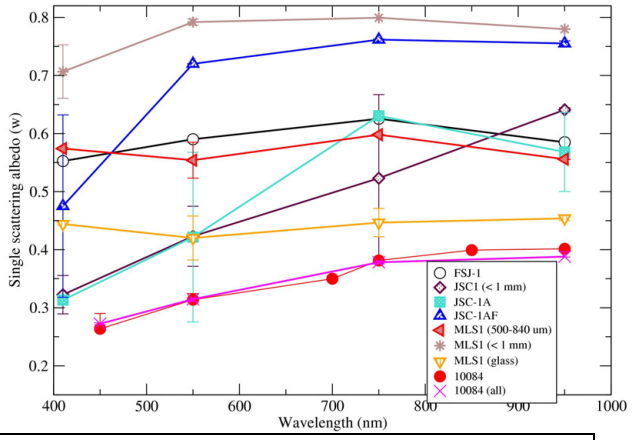

Figure 2. *w* values from 2-term HG models for 10084 soils modeled from standard BUG geometries (red circles) compared to values modeled from expanded geometries (magenta Xs) and model results for analog soils from [5].

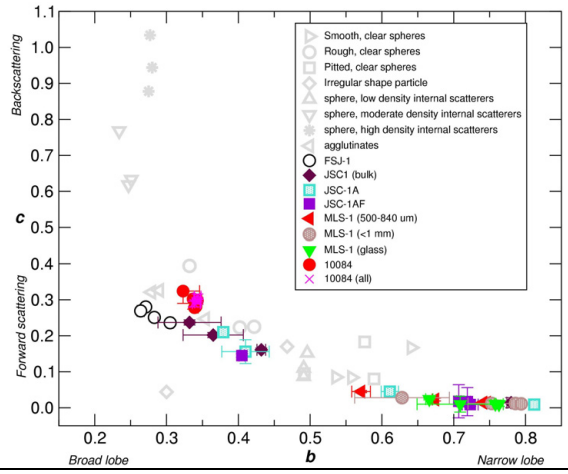

Figure 3. 2-term HG phase function values for 10084 soil modeled from standard (red circles) and expanded BUG geometries (magenta Xs), compared to analog soils [5] and synthetic particles [13].